bias voltage of 60.4, 67.2, and 74.5 V for the feed point (T) of 0.0043, 0.0044, and 0.0045 m, respectively. The radiation pattern of IMPATT diode loaded patch is shown in Figure 9. The radiation pattern indicates that the radiated power is decreases from -9.251×10^{-3} dB to -9.254×10^{-3} dB as the reverse bias voltage decreases from 80 to 55 V. However there is no major variation in radiation pattern with the bias voltage. However theoretical and simulated result show relatively good agreements. Therefore it is expected that performance of the antenna will remain satisfactory for the entire range of tunability.

REFERENCES

1. B.K. Kanaujia and B.R. Vishvakarma, Analysis of Gunn integrated annular ring microstrip antenna, IEEE Trans Antennas Propagat 52 (2004), 88–97.
2. S.K. Sharma and B.R. Vishvakarma, MOS capacitor loaded frequency agile antenna, Int J Electron 86 (1999), 979–990.
3. A. Nayak and B.R. Vishvakarma, IMPATT integrated active microstrip Antenna, Indian J Radio Space Phys 29 (2000), 357–362.
4. S. Srivastava and B.R. Vishvakarma, Tunnel diode loaded rectangular patch antenna, IEEE Trans Antennas Propagat 51 (2003), 750–755.
5. K.A. Hummer and K. Chang, Spatial power combining using active microstrip patch antennas, Microwave Opt Technol Lett (1988), 8–9.
6. H. Ohmine, Y. Sunahara, and M. Matsunaga, An annular-ring microstrip antenna fed by a co-planer feed circuit for mobile satellite communication use, IEEE Trans Antennas Propagat 45 (1997), 1001–1008.
7. S.Y. Liao, Microwave device and circuits, Prentice-Hall, India, New Delhi, 1992, pp. 68, 74, 311.
8. S.M. Sze, Physics of semiconductor device, Wiley, New York, 1969.
9. J.R. James and Hall, Handbook of microstrip antenna, Peter Peregriniyus, 1989, pp. 173, 174, 177.
10. H.K. Gummel and J.L. Blue, A small-signal theory of avalanche noise in IMPATT diodes, IEEE Trans Electron Dev (1967), 569–580.
11. Zeland software Co. IE3D 11.15, California, USA.

PRINTED-CIRCUIT FILTERS FOR WIRELESS DUAL- AND TRIPLE-BAND APPLICATIONS

K. Rambabu,[1] Adrian E. C. Tan,[2] Michael Y. W. Chia,[2] and Jens Bornemann[3]
[1] Department of Electrical and Computer Engineering, University of Alberta, Edmonton, AB, T6G 2V4, Canada
[2] Institute for Infocomm Research, 20 Science Park Road, 02-21/25 TeleTech Park, Singapore 117674
[3] Department of Electrical and Computer Engineering, University of Victoria, Victoria, BC, V8W 3P6, Canada; Corresponding author: j.bornemann@ieee.org

ABSTRACT: *Simple dual- and triple-band printed-circuit filters for wireless applications are presented. By using a single dual-behavior resonator for each individual band, two transmission zeros between passbands are obtained, thus providing high levels of rejection. Moreover, there is no limit on the ratio of highest to lowest passband. Several measured prototype performances show very good agreement with computations.* © 2008 Wiley Periodicals, Inc. Microwave Opt Technol Lett 50: 1495–1497, 2008; Published online in Wiley InterScience (www.interscience.wiley.com). DOI 10.1002/mop.23408
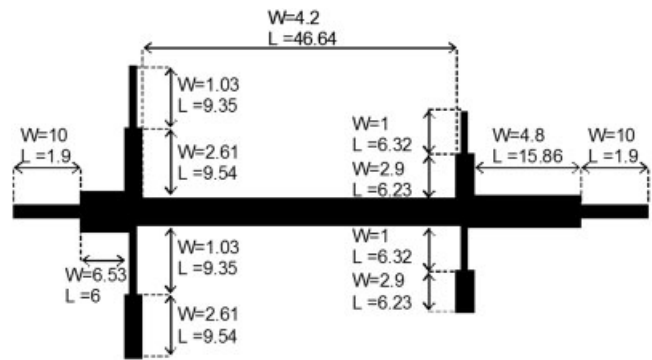
Figure 1 Principle layout of a dual-band filter; $å_r$=3.38, substrate thickness = 32 mils; dimensions in mm

1. INTRODUCTION

Modern telecommunication systems are required to operate in multiple frequency bands and have created a heavy demand for advanced RF filter designs. In the emerging standards for fixed broadband wireless access, such as IEEE 802.16 (or WIMAX),
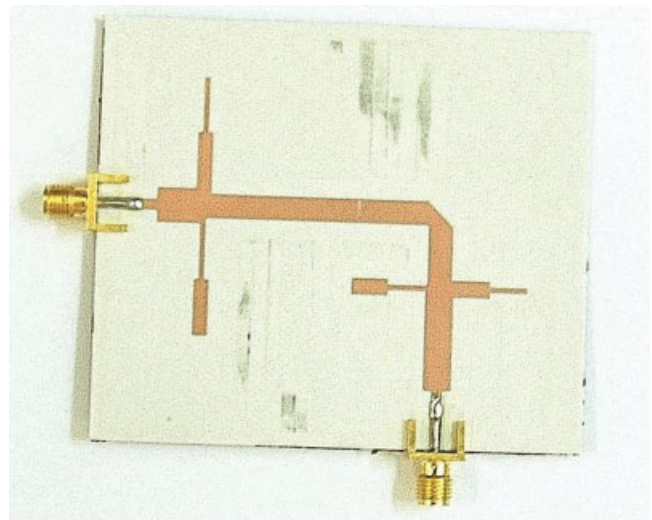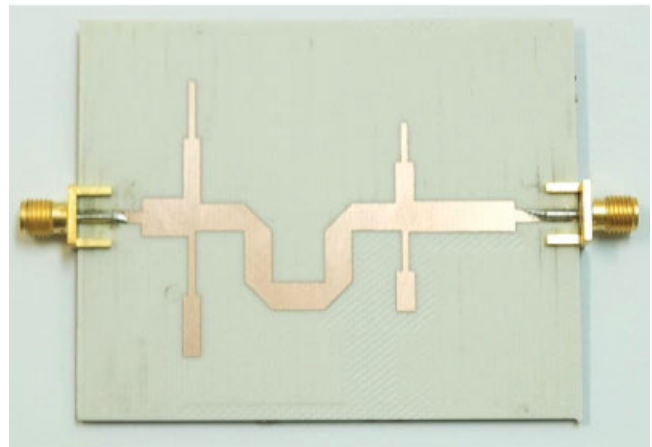
Figure 2 Photographs of dual-band filter prototypes with bent (a) and meandered (b) connections. [Color figure can be viewed in the online issue, which is available at www.interscience.wiley.com]

multiple bands are allocated below 11 GHz for non-line-of-sight operations [1]. Typically, most of the preferred licensed bands operate below 5 GHz, and several attempts have been made to accommodate different frequency bands in filter topologies.

To achieve multiband performance, individual filters can be connected in parallel. Such a component for 0.9 and 1.9 GHz is presented in [2], using a ceramic lamination technique. If used in regular printed-circuit technologies, however, this approach increases size and complexity. Therefore, recent single-input and single-output dual-band filter designs incorporate stepped-impedance resonators (SIR's), for example, [3–5]. But the design of SIR filters, especially in triple-band operation, is not necessarily straightforward.

A different methodology for multiband filter design consists of using stepped-line stubs to create transmission zeros for the separation of frequency bands. This approach led to so-called dual-behavior resonators (DBRs), for example, [6–8]. An application of this concept related to WLAN and UWB coexistence is presented in [9].

In this article, we present DBR dual-band filters in the licensed bands 2.1–2.3 GHz and 3.1–3.6 GHz for wireless application. Moreover, a triple-band filter additionally includes the 5.4 GHz ISM band for IEEE 802.16. Note that the bandwidths for the applications investigated here are small enough for the use of single-pole filters. In that respect, the filter designs presented here differ from those in [8] and [9], where the change/tuning of a single DBR influences all other passbands. In our design approach, each passband is separately designed and put together through transmission lines. Thus, no limit is put on the ratio of highest to lowest passband, and two transmission zeros between two neighboring passbands can always be obtained.

2. DESIGN

DBRs are realized by shunt-connecting two different open-ended stubs to a transmission line. Fundamental principles of DBR operation and basic design guidelines have been presented in [6, 7], and will not be repeated here.

Using these guidelines for two or three different frequency bands will place transmission zeros at the designed frequencies. Since the frequency characteristics of DBR's depend on the impedance ratio of
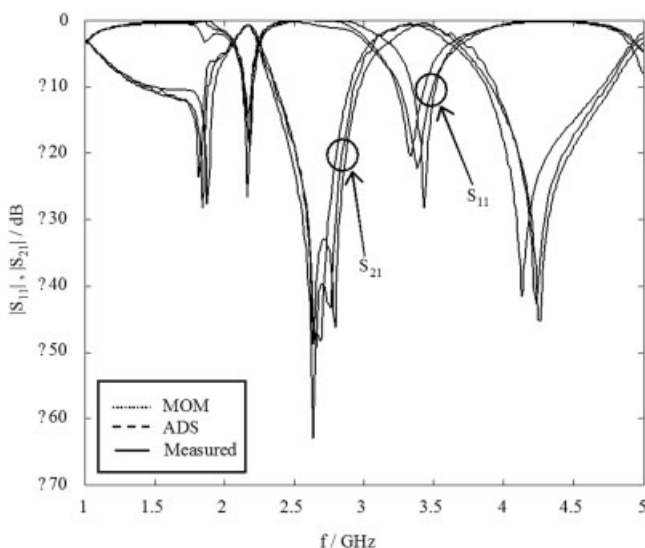
Figure 3 Comparison between computed (ADS and Momentum (MOM)) and measured results for the bent prototype of Figure 2(a)
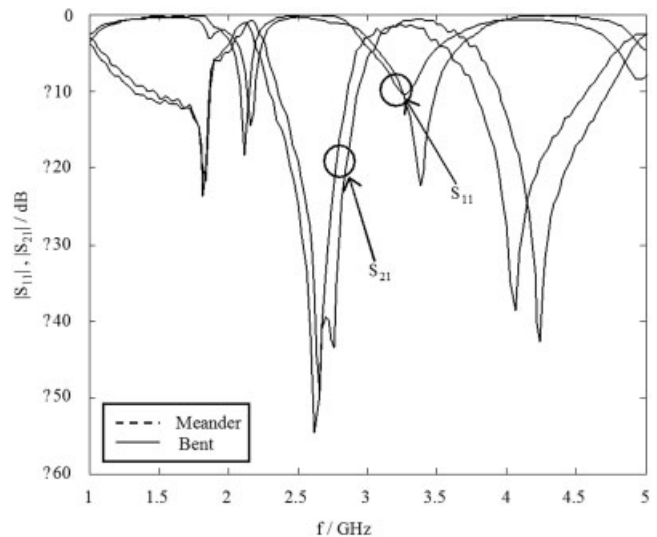
Figure 4 Comparison between measured responses of the two different dual-band filter prototypes

the sections and not on the absolute values of the impedances, it is advisable to select one of the impedances of the segments such that the other impedance determined from the impedance ratio is also in the practical range of printed-circuit technology (i.e., 20–80 Ω). By changing the impedance ratio, however, the center frequency will be shifted and, therefore, the lengths and impedances of the segments must be adjusted in a practical design. Note that the bandwidth of the DBR increases due to the low quality factor of the microstrip resonators, and that the locations of transmission zeros above the passband move toward higher frequencies. Observing this dependence in cascaded DBR's allows the placement of two transmission zeros between individual passbands.

For dual- and triple-band operation, the DBR's are initially connected through 50 Ω transmission lines, whose lengths are a quarter wavelength at a frequency half way between the two passbands. The circuit is then optimized to specifications using ADS software and cross-checked with the full-wave analysis tool Momentum. The discrepancy in the frequency responses between ADS and Momentum simulations is corrected by considering the percentage frequency shift in the individual passbands and tuning the lengths of the respective DBR and transmission-line sections.

3. RESULTS

3.1. Dual-Band Filter

Figure 1 shows the layout of a dual-band filter for the frequency ranges 2.1–2.3 GHz and 3.1–3.6 GHz. The transmission zeros for the first and second DBR's are 1.7, 2.7, and 2.8 GHz, 4.2 GHz, respectively. Note that the length between the two DBR's can—theoretically—be reduced by a full wavelength. However, this reduces the distance between the two DBR's to a point where coupling occurs.

To reduce the actual size of this filter, a bent and a meandered design are considered. The respective prototypes are shown in Figures 2(a) and 2(b). For the bent prototype of Figure 2(a), a comparison between the predicted performances (with both ADS and Momentum (MOM)) and measurements is depicted in Figure 3. Very good agreement is obtained, thus verifying the design procedure. Because of the two transmission zeros between the two passbands, the DBR's demonstrate excellent stopband performance, and rejection levels of 30–40 dB can be achieved. The agreement between measurements and computations is better in
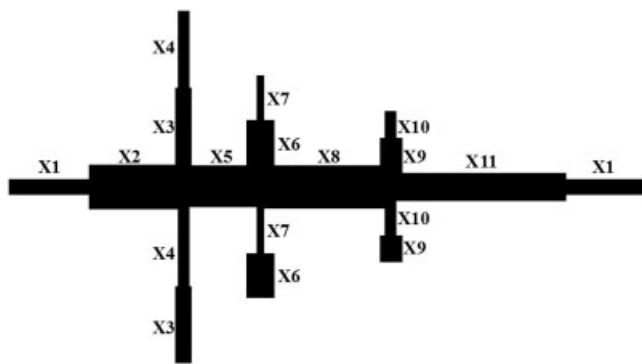
Figure 5 Layout and dimensions (width × length in mm) of the triple-band filter prototype: X1 = 1.9 × 10, X2 = 5.4 × 12.33, X3 = 2.2 × 9.47, X4 = 1.3 × 9.42, X5 = 5.1 × 6.76, X6 = 3.6 × 5.64, X7 = 0.9 × 5.6, X8 = 5.5 × 13.56, X9 = 3 × 3.32, X10 = 1.55 × 3.3, and X11 = 2.7 × 21.51; ε_r = 3.38, substrate thickness = 32 mils

the lower frequency range. This is also observed in the triple-band filter response presented in the next section, and is mainly attributed to manufacturing tolerances.

Figure 4 shows a comparison between the measured responses of the bent [Fig. 2(a)] and meandered [Fig. 2(b)] prototypes. They agree reasonably well, except for a small frequency shift that we attribute to the influence of the four bends (meandered) compared to just a single bend for the bent connection. The measured insertion losses in the two bands are 0.77 dB at 2.2 GHz and 0.6 dB at 3.4 GHz.

3.2. Triple-Band Filter

Figure 5 shows the layout and dimensions of a triple-band filter, which adds the 5.4 GHz ISM band to the dual-band filters discussed above. A comparison between the measured and computed responses (with both ADS and Momentum) is shown in Figure 6. Good agreement is demonstrated, and rejection levels better than 30 dB are obtained due to the placement of two transmission zeros between two passbands. The measured insertion losses in the three bands are 0.74 dB at 2.2 GHz, 0.91 dB at 3.4 GHz, and 1.7 dB at 5.4 GHz. A photograph of the triple-band filter prototype is shown in Figure 7.
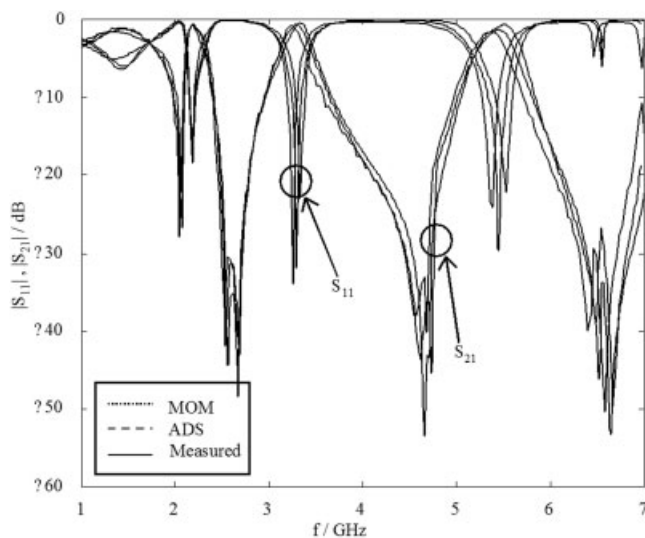
Figure 6 Measured and simulated responses of the triple-band filter prototype
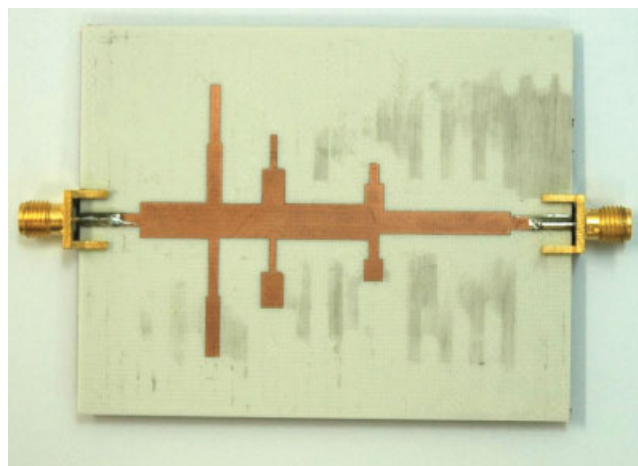
Figure 7 Photograph of the triple-band filter prototype. [Color figure can be viewed in the online issue, which is available at www.interscience.wiley.com]

4. CONCLUSIONS

The dual- and triple-band printed-circuit filters presented in this article are well suited for wireless applications. Each DBR creates one reflection and two transmission zeros. This allows two transmission zeros to be placed between two passbands and, therefore, high rejection levels can be achieved without restrictions on the ratio of highest to lowest passband. The design procedure involves circuit-level and full-wave simulations. It is verified by two dual-band and one triple-band filter prototypes that operate in licensed and ISM bands for IEEE 802.16.

REFERENCES

1. IEEE Std 802.16-2004, "IEEE standards for local and metropolitan networks, Part 16 Air Interface for fixed broadband wireless access systems", 24th June 2004, IEEE-SA Standards Board.
2. H. Miyake, S. Kitazawa, T. Ishizaki, T. Yamoda, and Y. Nagatomi, "A miniaturized monolithic dual band filter using ceramic lamination technique for dual mode portable telephones," in IEEE MTT-S International Microwave Symposium Digest, Denver, CO, 1997, pp. 789–792.
3. C.-H. Lee, C.-I.G. Hsu, and H.-K. Jhuang, Design of a new tri-band microstrip BPF using combined quarter-wavelength SIRs, IEEE Microwave Wireless Comp Lett 16 (2006), 594–596.
4. M.-H. Weng, H.-W. Wu, and Y.-K. Su, Compact and low loss dual-band bandpass filter using pseudo-interdigital stepped impedance resonators for WLANs, IEEE Microwave Wireless Comp Lett 17 (2007), 187–189.
5. Y.P. Zhang and M. Sun, Dual-band microstrip bandpass filter using stepped-impedance resonators with new coupling schemes, IEEE Trans Microwave Theory Tech 54 (2006), 3779–3785.
6. C. Quendo, E. Rius, and C. Person, narrow bandpass filters using dual-behavior resonators, IEEE Trans Microwave Theory Tech 51 (2003), 734–743.
7. C. Quendo, E. Rius, and C. Person, Narrow bandpass filters using dual-behavior resonators based on stepped-impedance stubs and different-length stubs, IEEE Trans Microwave Theory Tech 52 (2004), 1034–1044.
8. C. Quendo, E. Rius, A. Manchec, Y. Clavet, B. Potelon, J.-F. Favennec, and C. Person, "Planar tri-band filter based on dual behavior resonator (DBR)," in Proceedings of the 35th European Microwave Conference, Paris, France, 2005, pp. 269–272.
9. M.-L. Lai and S.-K. Jeng, A microstrip three-port and four-channel multiplexer for WLAN and UWB coexistence, IEEE Trans Microwave Theory Tech 53 (2005), 3244–3250.